Hindawi
Journal of Chemistry
Volume 2022, Article ID 3616050, 13 pages
https://doi.org/10.1155/2022/3616050

Research Article

Treatment of Wastewater from Thermal Desorption for Remediation of Oil-Contaminated Soil by the Combination of Multiple Processes

Feng Xiao,[1,2] Jun Yin ,[1,2] Dongsheng Shen,[1,2] Ting Chen,[1,2] and Li Lv[1,2]

[1]*School of Environmental Science and Engineering, Zhejiang Gongshang University, Hangzhou 310012, China*
[2]*Zhejiang Provincial Key Laboratory of Solid Waste Treatment and Recycling, Hangzhou 310012, China*

Correspondence should be addressed to Jun Yin; jun.yin77@gmail.com

Received 12 April 2022; Revised 8 September 2022; Accepted 30 September 2022; Published 18 October 2022

Academic Editor: Andrea Penoni

Thermal desorption (TD) is one of the methods commonly used to remediate contaminated soil. However, as water is the liquid adsorbent of the off-gas treatment system in the TD stage, the wastewater generated after multiple cycles in the TD stage has low biodegradability and contains complex organic pollutants. In addition to petroleum hydrocarbon, there are also a lot of ammonia, emulsified oil, phenols, aldehydes, and ketones. In this study, effective removal of contaminants was achieved using a combined process of demulsification and flocculation (DF), ammonia stripping (AS), Fenton oxidation (FO), and reverse osmosis (RO). The combined process was optimized, and the maximum chemical oxygen demand (COD), NH_3-N, turbidity, and extractable petroleum hydrocarbons (EPH) removal efficiencies reached 93.3%, 79.8%, 97.6%, and 99.9%, respectively. The FO was the key process for the efficient removal of contaminants. Ultraviolet-visible (UV/Vis), excitation-emission matrix (EEM), fluorescence spectroscopy, and gas chromatography-mass spectroscopy (GC-MS) showed that refractory macromolecular organic pollutants in water were removed, especially aromatics, phenols, and conjugated aldehydes or conjugated ketones, and further ring cleavage of benzene rings and carbocycles with carbon double bonds was observed. The cost-benefit analysis of the combined process was also carried out. The operating cost was 8.73 US$/m^3, indicating that the combined process involved moderate costs for recalcitrant wastewater treatment. No studies have been published on combined processes for the treatment of wastewater from TD for the remediation of oil-contaminated soils. Therefore, this study could provide fundamental information based on experimental results and guidelines for wastewater treatment in engineering applications.

1. Introduction

In the process of oil field exploitation, a particularly serious ecological problem is soil pollution by crude oil. There are large amounts of oil-contaminated soils in major oil fields worldwide, such as those in the Middle East, North America, western Africa, and East Asia [1]. A bulletin issued by the Chinese government showed that the main pollutants in oil-contaminated soils are volatile and semi-volatile pollutants represented by petroleum hydrocarbons and polycyclic aromatic hydrocarbons [2]. Because thermal desorption (TD) is suitable for the treatment of most volatile and semi-volatile contaminants, it has been widely used as a common remediation method for oil-contaminated soils. This method exhibits several advantages, such as the capability to treat different types of contaminants, short treatment period, high efficiency, high safety, lack of secondary pollution, and recycling of soil and contaminants [3]. However, contaminants in soil are volatilized during the TD stage and are transported to the off-gas treatment system by carrier gas. The main contaminants in off-gas include gaseous contaminants (such as VOCs and SVOCs) and pyrolysis products of soil organic matter. These contaminants could go into the liquid phase at the condenser or/and condensing scrubber, and wastewater from thermal desorption for remediation of oil-contaminated soil, i.e., the thermal desorption wastewater (TDW), is produced.

After oil removal by an oil/water separator, TDW still poses a serious threat to the ecological environment and human health. Due to the continuous circulation of the liquid absorbent produced by the spray in the TD system, TDW from the remediation of oil-contaminated soil has a complex mixture of pollutants, such as petroleum hydrocarbons and surfactants, which causes a high degree of toxicity and emulsification. The biodegradability of TDW is very poor, and it is difficult to be treated. Therefore, the treatment of site-specific TDW remains a major challenge.

Many unit processes for the treatment of oil-containing wastewater have been reported in previous studies, including the following unit treatment processes: pretreatment, secondary treatment, and advanced treatment [4]. The purpose of pretreatment is to remove suspended solids and oil from water to reduce the burden of the subsequent treatment, usually including demulsification-flocculation [5], coagulation-flocculation [6, 7], air stripping [8], and dissolved air flotation [9]. However, the effect of pretreatment on the removal of recalcitrant organics from water is limited, and a subsequent secondary and/or advanced treatment is required. Therefore, effective treatment requires complete mineralization of these recalcitrant pollutants. This can be achieved using advanced oxidation processes (AOPs), which can effectively oxidize organic pollutants in the secondary treatment [10]. Compared with other AOPs, the Fenton process is the most popular oxidation process because of its exciting advantages such as wide application range, strong anti-interference ability, simple operation and rapid degradation, and mineralization [11]. But Fenton oxidation suffers some limitations that hinder its large-scale applications. In addition to the high cost of treatment, the inability to completely remove micropollutants is also one of the main problems [12, 13]. Therefore, to reduce the operating cost of the Fenton process and further improve the treatment effect, it needs to be combined with other treatment processes. As a kind of advanced treatment, biological treatment is also widely used as a follow-up process of Fenton treatment [14]. However, it is not suitable for practical thermal desorption engineering because of the long-term acclimation of biological treatment. The main advantage of membrane technology as an advanced treatment is that it generates stable water without the addition of chemicals, with relatively low energy use, and is an easy and well-arranged process [15]. Membrane technology is widely used in petrochemical, power generation, and steel industries due to its excellent performance, while reverse osmosis (RO) has the best separation performance among all membrane technologies [16]. However, there are some limitations in the operation of RO, such as the need for strict inlet water quality [17]. If membrane technology is used directly for oily wastewater, membrane pollution will seriously reduce the treatment efficiency [18, 19]. Therefore, proper pretreatment has been stressed repeatedly as the first line of defense in controlling membrane fouling and assuring success for RO operation [20]. The Fenton process can be combined to improve the inlet water quality, reduce membrane pollution, improve the service life of membrane components, and reduce energy consumption and operating costs [21].

During the oil exploitation, some additives such as solvents, surfactants or inorganic salts, and water-soluble and oil-soluble polymers are used, so the wastewater in this study contains phenols, aldehydes, ketones, and ammonia, except for petroleum hydrocarbons. The configured unit process should be established according to the specific conditions and the physicochemical properties of the wastewater. Therefore, a combined process of demulsification and flocculation (DF), ammonia stripping (AS), Fenton oxidation (FO), and RO has been developed to remove oil, ammonia, chemical oxygen demand (COD), and small molecular organics. The operating parameters of each process were optimized. The fate and possible removal pathway of the pollutants in wastewater were determined. Also, the engineering applicability was evaluated, and the benefit analysis of the combined process was performed to provide alternative technologies for the effective treatment of wastewater from TD for oil-contaminated soils.

2. Materials and Methods

2.1. Materials. Iron (II) sulfate heptahydrate ($FeSO_4 \bullet 7H_2O$, ≥99%), hydrogen peroxide solution (H_2O_2, 34.5wt%), sulfuric acid (H_2SO_4, ≥98%), sodium hydroxide (NaOH, ≥99%), calcium chloride anhydrous ($CaCl_2$, ≥96%), and sodium hypochlorite solution (NaClO, Cl ≥ 5.2%) were purchased from Lingfeng; poly aluminium chloride (PAC, $Al_2O_3 \geq 28\%$) was purchased from Aladdin; polyacrylamide (PAM, cationic) was purchased from Macklin.

2.2. Thermal Desorption Wastewater. The TDW was collected from indirect thermal desorption for remediation of crude oil-contaminated soil in Tahe, Xinjiang, China. The wastewater is the liquid absorbent from the indirect thermal desorption treatment system. After a long recycling operation of water, the water contained high amounts of emulsified oil and was rich in refractory organic matter. The water was light brown, turbid, and had a pungent odor with high concentrations of COD, oil, and NH_3-N (see Figure S1 for an on-site water sample map). Table 1 shows the main water quality.

2.3. Experiments. DF experiments were performed using a jar test apparatus. Each sample to be coagulated was added with NaClO and placed under a state of rapid stirring (250 rpm). $CaCl_2$ was slowly added after stirring for 60 s. After adding PAC, the flocculant was stirred slowly for 5 min at a speed of 50 rpm. At the last stage, PAM was added to make the flocculant settle for 30 min. The supernatant obtained after settling was subjected to analysis.

AS experiments were conducted by placing the supernatant after DF in a 500 mL Erlenmeyer flask, and spherical aeration heads were installed inside, through which external air could be supplied. The air required for stripping was controlled at a pressure of <30 Pa using a blower and regulator, and a flow meter was used to control the volume. The

Table 1: Main water characteristics parameters of wastewater from TD of oil-contaminated soil in Tahe, Xinjiang, China.

Parameters	Value	Parameters	Value
COD	9724 (mg/L)	As	92.1 (μg/L)
NH_3-N	252 (mg/L)	Hg	1.37 (μg/L)
Turbidity	596 (NTU)	Cu	0.02 (mg/L)
Oil content	1377 (mg/L)	Cr	0.06 (mg/L)
Petroleum hydrocarbons	818 (mg/L)	Mn	1.01 (mg/L)
pH	7.8	Se	2.5 (μg/L)

change in ammonia concentration in wastewater was observed by changing pH, temperature, time, and aeration rate.

FO experiments were conducted on the AS effluent and putting it into a wide mouth bottle. A fixed volume of 250 mL of wastewater was fed into the reactor and the desired amount of $FeSO_4 \cdot 7H_2O$ was transferred to the reactor after adjustment to the corresponding pH with H_2SO_4 (2 mol/L). To initiate the reaction, H_2O_2 was introduced under constant stirring at 150 rpm (to homogenize the mixture). Thereafter, the reaction was terminated by spiking the sample with NaOH (2 mol/L), which adjusted the pH of the solution to above 10.0. This resulted in decomposing residual H_2O_2 and precipitation of the iron as $Fe(OH)_3$ which was then filtered using a 0.45 μm filter. Lastly, the supernatant was used for COD, oil concentration, and petroleum hydrocarbon analyses.

RO experiment was performed using FlowMem-0021-HP equipped with Dow SW30-2514 RO membrane (maximum operating pressure: 800 (55) psig (ber); seepage discharge: 150 (0.6) gpd (m^3/d); pH range suitable: 1.0–12.0). By pouring FO effluent into a bucket, the pressure was slowly raised to 6 MPa. The filtrate passes through the RO membrane in the device and is collected in the discharge bottle for subsequent analysis.

The orthogonal experimental design tables are shown in the Supplementary Materials (Tables S1–S3). All experiments were carried out using wastewater from the contaminated site in Tahe, Xinjiang, China, and the process flow is shown in Figure S2.

2.4. Analysis. COD was measured via a HACH DRB200 coupled with a DR1010 attachment, and a turbidimeter (SGZ-200A) was used to measure turbidity. NH_3-N was determined by indophenol blue spectrophotometry [22]. The oil concentration of the permeate solutions was recorded using a UV-vis spectrophotometer (UV2600 A, China) based on an absorbance wavelength of 225 nm. Liquid n-hexane was used as the solvent to extract oil from the filtrate [23].

Gas chromatography-flame ionization detection (GC-FID; Agilent GC-8890) was used to analyze extractable petroleum hydrocarbons (EPH) in water samples. The chromatographic column was an HP-5 column, the heating program was as follows: 60°C for 1 min and heating to 320°C for 5.5 min at a rate of 40°C/min; the injection port temperature was 300°C, and the detection temperature of the device was 305°C.

Ultraviolet-visible (UV-vis) spectra were recorded using a UV-2600i UV-vis spectrophotometer, with Milli-Q water as a blank, and a 1-cm quartz cuvette in the wavelength range of 200~500 nm.

The 3D-EEM spectra were performed over excitation wavelengths between 200 and 450 nm in 10 nm intervals and emission wavelengths ranging from 280 to 550 nm in 10 nm intervals.

Gas chromatography-mass spectroscopy (GC-MS; GC-MS2020NX) was used to identify the compounds. The instrument was equipped with a DB-5MS column, the heating program was as follows: 60°C for 1 min and followed by a ramp at 10°C/min to 280°C, and a ramp at 5°C/min to 300°C, which was held for 4 min; the injection port temperature was 290°C, and the detection temperature of the device was 300°C.

3. Results and Discussion

3.1. Unit Process for TDW Treatment

3.1.1. Demulsification: Oil Removal. The TDW with a high oil content of 13.8% (w/w) was an oil/water (O/W) emulsion, so various demulsifiers were used in this study. NaClO, $CaCl_2$, PAC, and PAM were added successively. NaClO can destroy the close adhesion of oil and water and assist the subsequent flocculation. Ca^{2+} collides with the oil-water interface film and destroys the stability of the oil-water mixture. At the same time, Ca^{2+} adsorbs the tiny negatively charged oil particles in the emulsion and compresses the electric double layer of these particles. Demulsifiers work by surrounding the interfacial film around the droplets, and in doing so change the rheological property of the film by gradually weakening until it collapses leading to the aggregation and coalescence of the dispersed droplets. As the droplets coalesce, their size increases until the eventual separation of the phases [24]. PAC and PAM play the role of coagulators to further remove suspended pollutants from water. After adding NaClO, $CaCl_2$, PAC, and PAM in sequence, large flocs precipitated, and the turbidity decreased significantly from 596.0 NTU to 14.3 NTU (Figure S3). Table 2 shows the settling velocity, turbidity, layered effect, floc size, and COD removal after adding NaClO, $CaCl_2$, PAC, and PAM.

The orthogonal test results showed that under the conditions of 20 mL/L NaClO, 6 g/L $CaCl_2$, 6 g/L PAC, and 3 g/L PAM, the oil removal efficiency was the highest at 65.3%, the removal efficiencies of turbidity and COD were 97.6% and 15.3%, respectively (Table S1). The results showed that DF could efficiently remove the turbidity of wastewater, which greatly reduces the burden of subsequent treatment. The low COD removal efficiency was mainly because the water contained high amounts of refractory organic matter, which cannot be removed. Yang et al. [25] also found that low doses of coagulants and flocculants were insufficient to destroy the stability of all colloidal particles, so it is necessary to add enough demulsifier and flocculants for wastewater with high COD and oil contents. Yao et al. [26] found that after the addition of 5 g/L $CaCl_2$, 4 g/L PAC, and 0.02 g/L

Table 2: Settling velocity, turbidity, layered effect, floc size, and COD removal after adding NaClO, $CaCl_2$, PAC, and PAM.

N#	Water sample	Settling velocity	Turbidity	Layered effect	Floc size	COD (mg/L)
1	TDW	—	Muddy	Not obvious	No floc	9724
2	TDW, NaClO	Slow	Muddy	Not obvious	Smaller floc	9636
3	TDW, NaClO, $CaCl_2$	Slow	Relatively turbid	Layered	Slightly larger floc	9480
4	TDW, NaClO, $CaCl_2$, PAC, PAM	Fast	Relatively clear	Layered	Larger floc	8239

APAM (anionic polyacrylamide), COD concentration of oily wastewater decreased from 36,270 mg/L to 29,054 mg/L, indicating that DF has a limited COD removal efficiency. In addition, Das and Somasundaran [27] reported that in addition to electrostatics, other forces (such as hydrogen bond bridging) between polymer flocculant and particles were also responsible for the flocculation. Therefore, too large amounts of acid or alkali are not conducive to the treatment of oily wastewater. Thus, in the experiment, to save costs and ensure the removal effect, the wastewater can be kept neutral, without additional adjustment of pH.

3.1.2. Ammonia Nitrogen Removal. After DF treatment, the PH of effluent is about 8.5–9.0, and the turbidity and oil content of effluent are greatly reduced, but the ammonia nitrogen and COD concentrations are still very high. Considering that AS needs to be in alkaline condition, and AS can not only effectively remove ammonia nitrogen but also has a certain ability to remove COD, which also reduces the burden for subsequent processing. Therefore, the wastewater after DF treatment was treated with AS, and the effects of pH, temperature, aeration rate, and treatment time on NH_3-N removal were verified (Figure 1). With the increase in the pH, the NH_3-N removal efficiency gradually increased. When the pH increased from 9.0 to 10.0, the removal efficiency increased sharply, and when the pH was 12.0, the NH_3-N removal efficiency reached 80%. As is well known that when the pH is alkaline, NH_3-N exists mainly as free ammonia (NH_3). By changing the equilibrium constant of the two nitrogen forms (NH_3-N and NH_4^+-N) in water, the percentage of NH_3 gas generation is increased, and NH_3-N removal is achieved by air stripping [28].

The NH_3-N removal efficiency gradually increased with an increase in the aeration rate. When the aeration rate was higher than 0.5 L/min, the NH_3-N removal efficiency reached 99.8% (Figure 1). An increase in aeration increases the diffusion driving force of NH_3-N in water and strengthens the desorption and mass transfer rate of NH_3-N from the liquid to the gas phase so that the removal efficiency is improved.

With an increase in the stripping temperature, the NH_3-N removal efficiency gradually increased and was greater than 90% at 55°C (Figure 1). AS is a mass transfer process, and the concentration of gas in the gas phase and liquid phase conforms to Henry's law, so the increase in temperature under certain pressure conditions can increase the diffusion coefficient of NH_3-N and reduce the solubility of NH_3-N in water [28, 29]. On the other hand, when the temperature was above 55°C, the rising trend of the NH_3-N removal efficiency gradually leveled off (Figure 1) because at this temperature the diffusion of NH_3-N in the gas-liquid two phases reaches equilibrium. Thus, the removal efficiency of NH_3-N does not increase anymore when the temperature continues to rise, but the energy consumption of the equipment greatly increases.

During the stripping process, gas is continuously discharged over time, which changes the ammonia concentration in the gas phase, so that the actual ammonia concentration is always lower than its equilibrium concentration, and the NH_3-N in the wastewater can be continuously removed. After 150 min, the NH_3-N removal efficiency increased slowly and finally reached 98.0% (Figure 1). At a pH of 10.0, a temperature of 70°C, and a treatment time of 70 min, the NH_3-N concentration decreased from 204 mg/L to 41 mg/L (Table S2).

3.1.3. Fenton Oxidation. After the processes of DF and AS, although the contents of oil, turbidity, and NH_3-N in water effectively decreased, COD concentration was still as high as 6160 mg/L, and a subsequent oxidation treatment process was still needed. As an advanced oxidation process, the Fenton reagent is suitable for the treatment of high-concentration organic wastewater that is difficult to biotreatment [30].

The degradation efficiency of organic pollutants during FO depends on operating parameters, such as wastewater pH, treatment time, and the dosage of H_2O_2 and Fe^{2+}. In Figure 2, the COD removal efficiency increased continuously with an increase in the dosage of H_2O_2. When the dosage of H_2O_2 was 1.0 mol/L, the COD removal efficiency reached 66.7%. When the Fe^{2+} dosage increased from 7 to 21 mmol/L, the COD removal efficiency increased from 58.4% to 65.8%, the COD concentration decreased to 2359 mg/L (Figure 2). However, when the Fe^{2+} dosage continued to increase to 35 mmol/L, the COD removal efficiency decreased slightly. According to the reaction mechanism, it is found that if Fe^{2+} is added in excess, a large number of active •OH will be generated very quickly with H_2O_2, while the reaction of •OH with the substrate is relatively slow so that unconsumed free radicals accumulate and interact with each other. The reaction generates water, causing a part of the •OH to be consumed, reducing the utilization rate of •OH, and excessive dosage of Fe^{2+} increases the color of the water [31, 32].

Figure 2 shows the relationship between COD removal efficiency and H_2O_2, Fe^{2+}, pH, and time. The decomposition rate of H_2O_2 varied with different pH. Under acidic conditions, the decomposition rate of H_2O_2 becomes slower, which is beneficial to the oxidation reaction. At the same time, the conversion of Fe^{2+} to $Fe(OH)_3$ can be achieved by

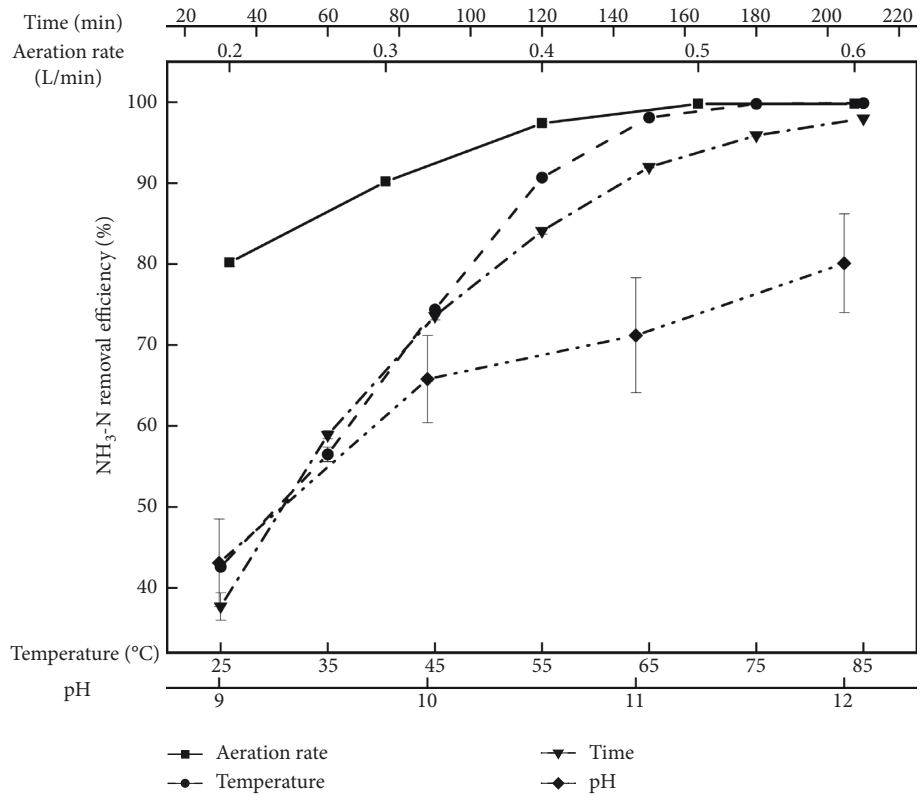

Figure 1: Relation of NH_3-N removal efficiency with pH, aeration rate, temperature, and time.

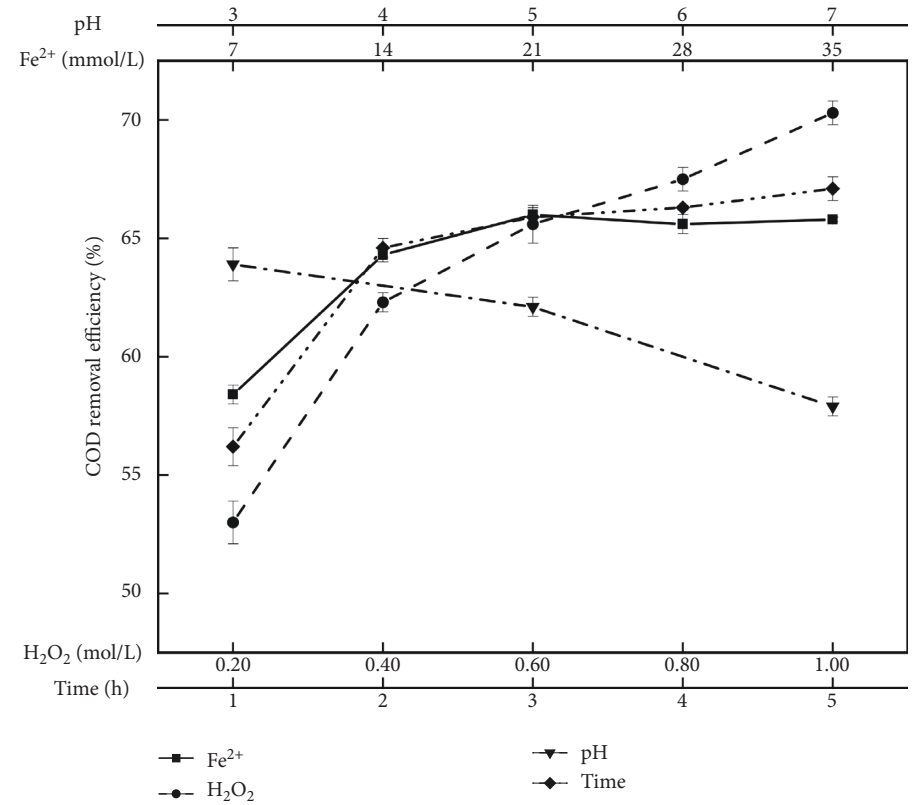

Figure 2: Relationship between COD removal efficiency and H_2O_2, Fe^{2+}, pH, and time.

adjusting the pH, and color and COD removal can be improved by coagulation/flocculation [33]. In Figure 2, the organic compounds in water were oxidized by HO• completely within the first 2 hours, and a further increase in the treatment time has little effect on the COD removal. The optimal COD removal efficiency was achieved at the pH of 3.0, the Fe^{2+} dosage of 32.4 mmol/L, the H_2O_2 dosage of 0.9 mol/L, and the treatment time of 5 h. Moreover, the reaction conditions and Fe^{2+}/H_2O_2 ratio in the experiment were within the appropriate range [34]. The COD decreased from 6160 mg/L after AS to 2250 mg/L (Table S3).

3.1.4. Reverse Osmosis. Because COD concentration in the effluent after FO was still higher than 2000 mg/L, the discharge standard was not met. According to the Fenton oxidation effluent, the organic pollutants in water were mainly small molecular matters such as ketones, aldehydes, carboxylic acids, and esters (Figure S5 and Table S5). Because RO provides smaller pore sizes (below 1 nm), it can effectively separate organic liquids (such as alkanes, alcohols, aromatics, and cyclic alkanes) [35]. Al-Huwaidi et al. [36] modeled and simulated the hybrid system of the RO process for the removal of phenol from wastewater. Pozderovic. et al [37] also investigated the influence of processing parameters and membrane types on permeate flux when reverse osmosis concentrates different alcohols, esters, and aldehydes and found that the permeate flux is lower in the concentration of alcohol and ester solutions of the higher molecular mass, a decrease of the permeate flux during the concentration is greater with greater alcohol molecular mass. In this study, FlowMem-0021-HP unit equipped with Dow SW30-2514 RO membrane for RO treatment of FO effluent. The pressure was controlled at 6 MPa, the COD concentration in the effluent was reduced to 150 mg/L, and the COD removal efficiency reached 93.3%, which met the second-class standard of Integrated Wastewater Discharge Standard of China (GB 8978–1996).

3.2. Removal of EPH. Figure 3 shows EPH removal in TDW at various process stages. After the combined DF, AS, FO, and RO process, EPH concentration decreased from 818 mg/L to 0.76 mg/L, and the removal efficiency was up to 99.9%. EPH was mainly removed in the DF and FO processes. The DF process effectively removed EPH, with a removal efficiency of 67.2%, and a reduction from 818 mg/L to 218 mg/L. The remaining EPH was completely removed in the FO process, after which the EPH concentration dropped to 1.24 mg/L, and the removal efficiency reached 99.8%. Previous studies on EPH degradation by means of oxidation have also been reported. Hassan [34] used the FO process to degrade Iraqi Petroleum Refinery Wastewater in experiments and determined that the optimal H_2O_2/Fe^{2+} molar ratio and treatment time were 15 and 60 min, respectively, the COD removal efficiency was 86%, and the petroleum hydrocarbon concentration decreased from 742 mg/L to 23 mg/L, corresponding to a removal efficiency of 97%. The combination of FO and bioremediation of petroleum hydrocarbon-contaminated soil could achieve a 55% petroleum hydrocarbon removal [38].

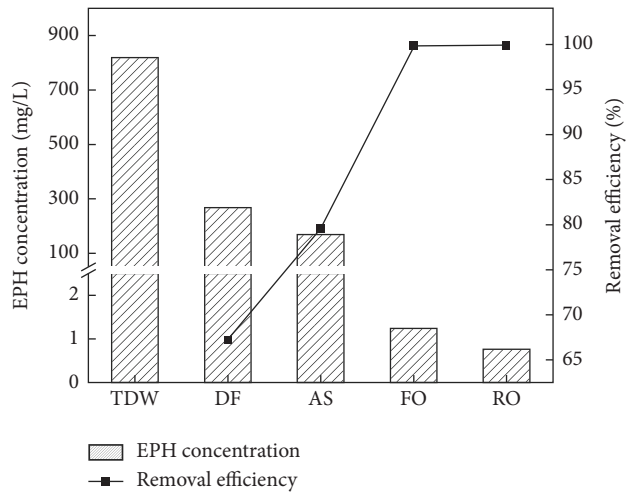

Figure 3: EPH concentration and removal efficiency of effluent from different processes.

3.3. Pollutant Degradation Analysis. First, the raw wastewater and the effluents from the DF, AS, and FO processes were characterized by UV-vis spectrophotometry. UV-vis can quickly obtain the characteristics of organic pollutants in wastewater. Figures 4 and 5 show the UV spectra of the effluents from each process and the calculation results of the corresponding parameters, respectively. In Figure 4, the UV-vis spectra of TDW did not show many absorption peaks, which indicates that there were many organic functional groups in the raw wastewater and little interference with each other. The raw wastewater, DF effluent, and AS effluent had obvious absorption peaks at 233 nm, indicating that there were many conjugated aldehydes or conjugated ketones in water; the absorption peak at 283 nm indicated that the water contained many phenols as well [39]. These two absorption peaks were absent in the effluent of FO. Based on the $A_{200\sim240}$ and $A_{240\sim400}$ parameters shown in Figure 5(a), the absorption peak and integral area of the FO effluent were greatly reduced, indicating that the organic matter in the water had been effectively removed in the FO process. In addition, the SUV_{254} and $A_{253/203}$ parameters of the effluents from each process were calculated (Figure 5(b)). The SUV_{254} value has been widely used as an indicator for evaluating the concentration of aromatics in water, and a SUV_{254} value < 0.4 represents a poor degradability of organic matter [40]. The SUV_{254} value decreased to below 0.4 after FO, indicating that the concentration of aromatics in water decreased, while the organic matter became more difficult to degrade. The $A_{253/203}$ ratio reflects the concentration of carbonyl, carboxyl, hydroxyl, and ester substituents, and its changing trend was similar to that of SUV_{254}. The results from SUV_{254}, $A_{253/203}$, $A_{200\sim240}$, and $A_{240\sim400}$ showed that the organics in the raw wastewater were in an aged state, that is, the molecular structure of the organics was complex, containing many aromatic compounds and hydroxyls. Substituents, such as carbonyl, carboxyl, and esters indicate that organics in water have high stability and are difficult to degrade [41, 42]. After FO treatment, organic compounds were obviously removed, especially aromatic species,

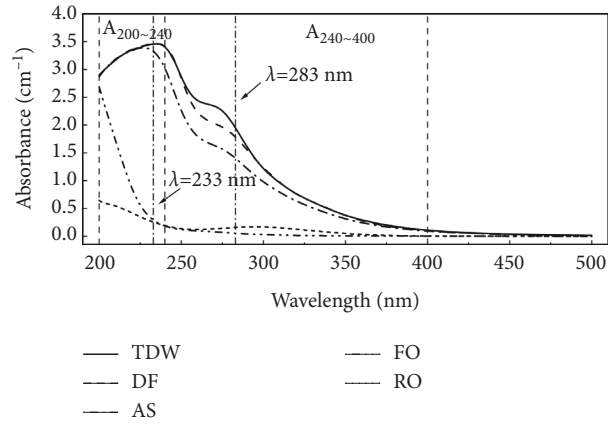

Figure 4: UV-vis spectra of the effluent from different processes.

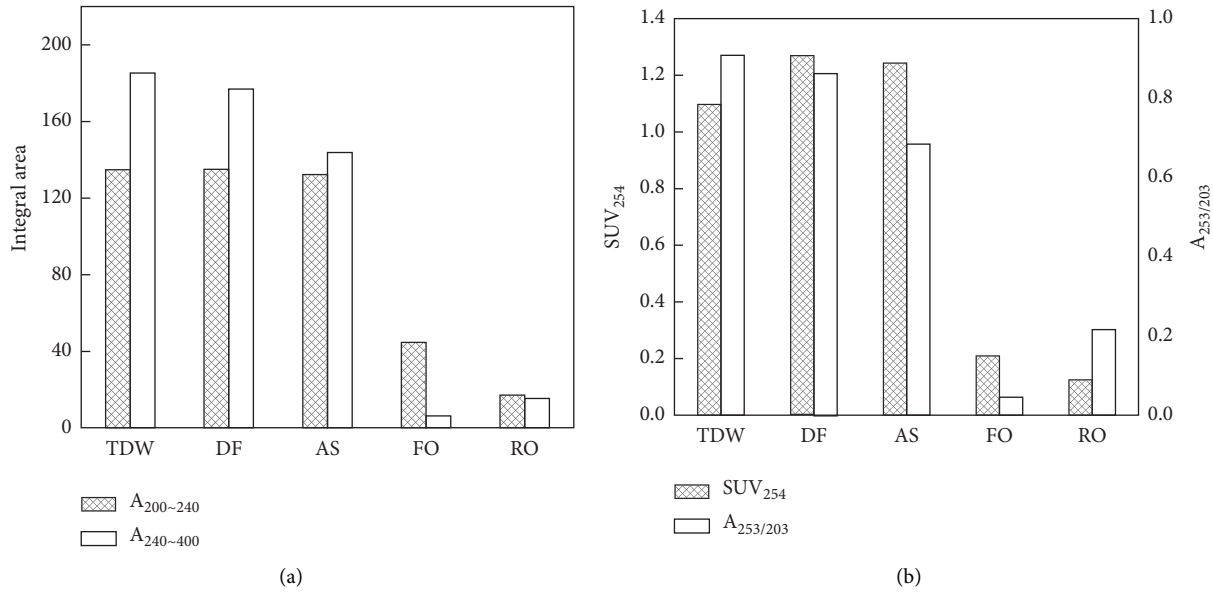

Figure 5: (a) Variation of the integrated area of absorbance at $A_{200\sim240}$ and $A_{240\sim400}$ of the effluent from different processes; (b) parameter variation of SUV_{254} and $A_{253/203}$.

phenols, and conjugate aldehydes or conjugate ketones. Comparing FO and RO, it can be found that the organic matter that cannot be completely degraded in FO is effectively removed in the RO stage (Figure 4).

UV-vis detection has certain limitations in terms of sensitivity and detection limit. By contrast, EEM fluorescence spectroscopy can play an important role in the detection and analysis of organic pollutants because it has multiple advantages, such as providing a highly comprehensive characterization and abundant fluorescence information, high sensitivity, fast detection speed, and good selectivity [43]. In Figure 6, EEM fluorescence analysis of the effluents from each process, P1, P2, P3, and P4 correspond to the fluorescence spectra of the raw wastewater, DF effluent, AS effluent, and FO effluent after 100-fold dilution, respectively. P5 is the fluorescence spectrum of FO effluent without dilution. The fluorescence spectrum in Figure 6 could be divided into five regions, in which regions I and II were located in the range of Ex/Em = (200~250) nm/(260~320) nm and Ex/Em = (200~250) nm/(320~380) nm; the ranges of regions III and IV were Ex/Em = (200~250) nm/(>380) nm and Ex/Em = (250~450) nm/(260~380) nm respectively, and region V was located at Ex/Em = (250~450) nm/(>380) nm [44]. Regions I and II are mainly easily degradable organic substances, mainly aromatic protein substances with a benzene ring structure, regions III and IV belong to the fluorescent region of degradable organic matter, and region V is the fluorescent region of refractory organic matter, for which macromolecular humic substances are the main host [45]. Based on Figure 6, P1, P2, and P3 were similar, the main peak appeared in region IV, and all other peaks appeared in regions I, III, and V, while the main peak in P4 was in region V, and there were no obvious peaks in other regions. These results indicate that the raw wastewater, DF effluent, and AS effluent contained complex organic compounds, and after FO, the organic compounds

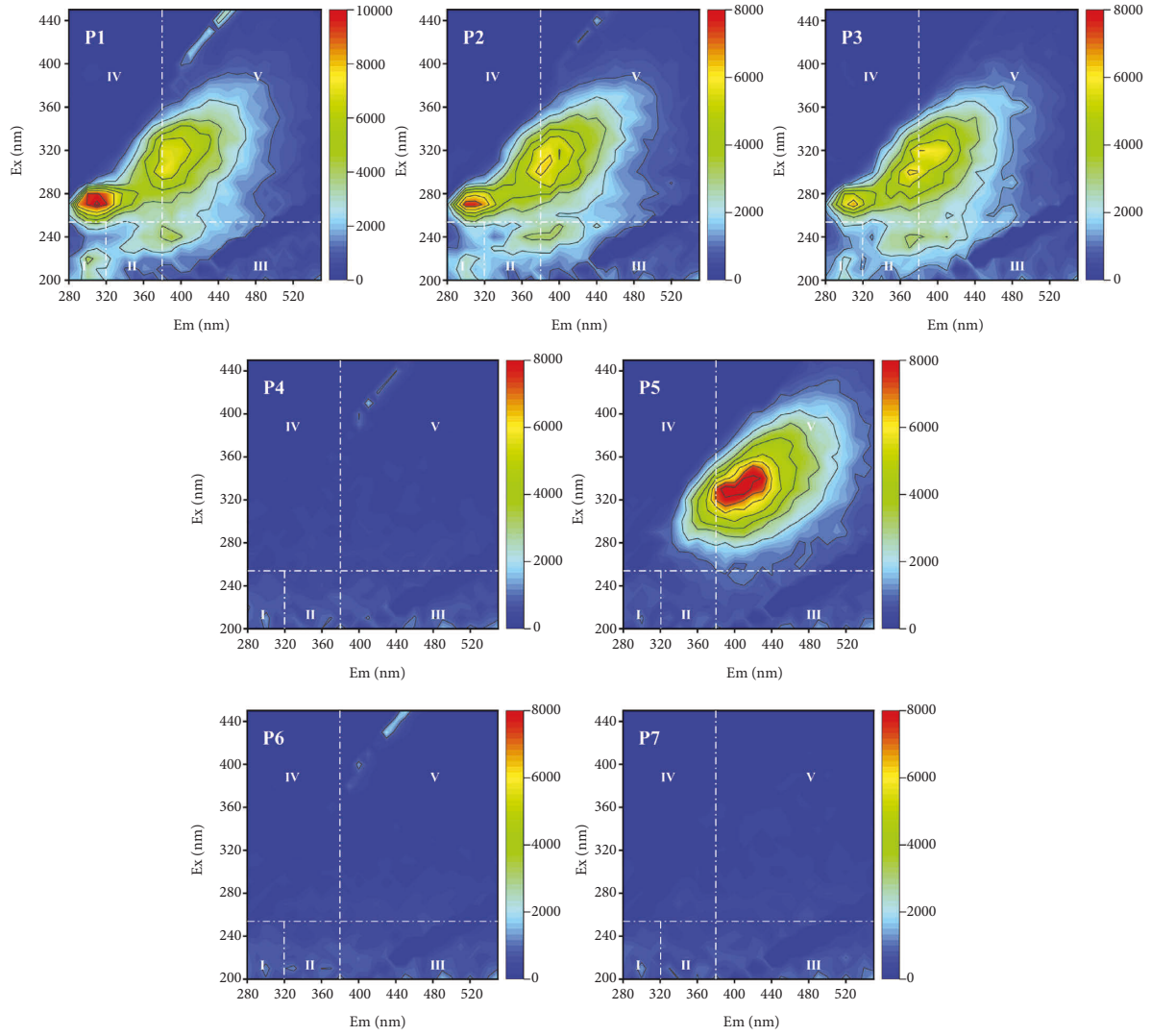

Figure 6: Typical EEM matrix of effluent from different processes (P1: raw wastewater, P2: DF, P3: AS, P4: FO, P5: no dilution FO, P6: RO, and P7: no dilution RO).

represented by regions I, III, and IV were almost completely removed. The refractory organics represented by region V were also effectively removed. Based on the fluorescence integration of the five regions (Figure 7), the integrated area decreased significantly after FO. Related research showed that the oxidation of Fe^{2+}/H_2O_2 mainly destroys the benzene ring structure and then generates unsaturated fatty acids with π^*-π conjugated double bonds [46]. Because the raw wastewater contained substances with benzene ring structure, after being oxidized, Fe^{2+}/H_2O_2 could further decompose unsaturated fatty acids, which was one of the reasons for the more thorough oxidation of organic matter. In addition, there were still fluorescent substances in region V of P4 and P5 (Figure 6), indicating that there were still some refractory organic substances that could not be degraded, and these refractory organic compounds were removed in RO (P6 and P7), which is consistent with the COD degradation results and UV-vis spectra.

Figure 8 shows the 3D-EEM of the raw wastewater. The characteristic peaks of phenols are in the vicinity of Ex/Em = 270/300 nm and Ex/Em = 220/300 nm, where C and *D* peaks in the region I were located [47], while other monocyclic compounds such as dichlorobenzene and benzene may also contribute to the C and *D* peaks [43]. The A peak located in region II may be related to bicyclic and tricyclic aromatic hydrocarbons. The fluorescence peaks near Ex/Em = 228/340 nm and Ex/Em = 256/363 nm at which the A peak was located are characteristic peaks of naphthalene and phenanthrene series [48]. In addition, the B peak located in region V generally exists in the fluorescence spectrum of various petroleum substances. Except for saturated hydrocarbons that do not fluoresce in petroleum components, other components involve a luminescence phenomenon, mainly polycyclic aromatic hydrocarbons, heterocyclic compounds, and benzene substances [49]. Peaks A and B located in regions IV and V are both

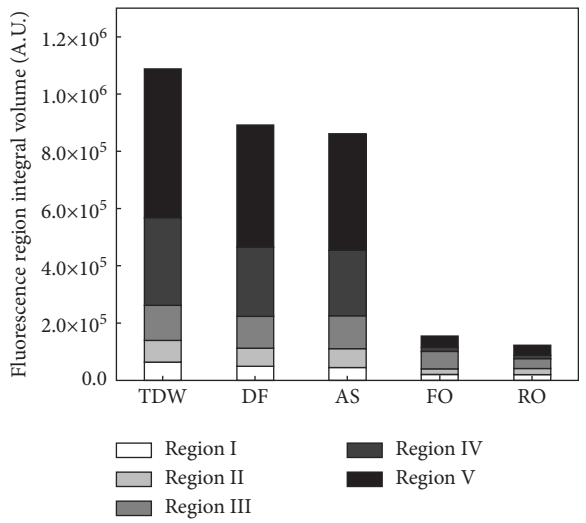

Figure 7: Fluorescence integral volume change of the effluent from different processes.

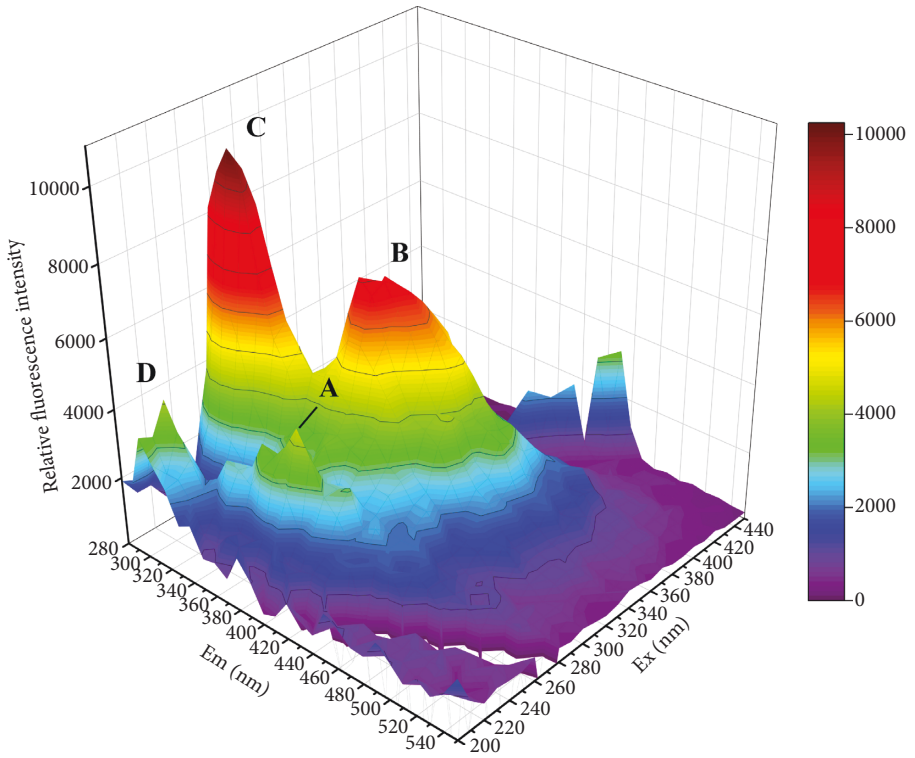

Figure 8: 3D-EEM of thermal desorption raw wastewater.

indicative of refractory macromolecular organics [50], which is also consistent with the UV-vis spectral analysis results.

Figure 9 shows the GC-MS total ion chromatogram of the raw wastewater and FO effluent. The peak area of organic matter in Figure 9(b) was greatly reduced compared with that in Figure 9(a), and the types of organic matter also changed significantly. Mass spectrometry analysis of the total ion chromatogram showed that phenolic organic compounds such as phenol, 3-cresol, and 2,3-dimethylphenol may have existed in the raw wastewater, in addition to 2-methyl-2-cyclopenten-1-one, 2,5-hexanedione, 5-methylfuran aldehyde, or 2,3-dimethyl-2-cyclopentenone. Degraded conjugated aldehydes or conjugated ketones were also present (Figure S4), which is consistent with the results of UV-vis spectroscopy and EEM fluorescence spectroscopy. However, there may have still been acetoxy-2-acetone, 2,5-hexanedione, 1,1,3-trichloroacetone, and other ketone organic compounds in the effluent of FO, indicating the presence of conjugated ketones

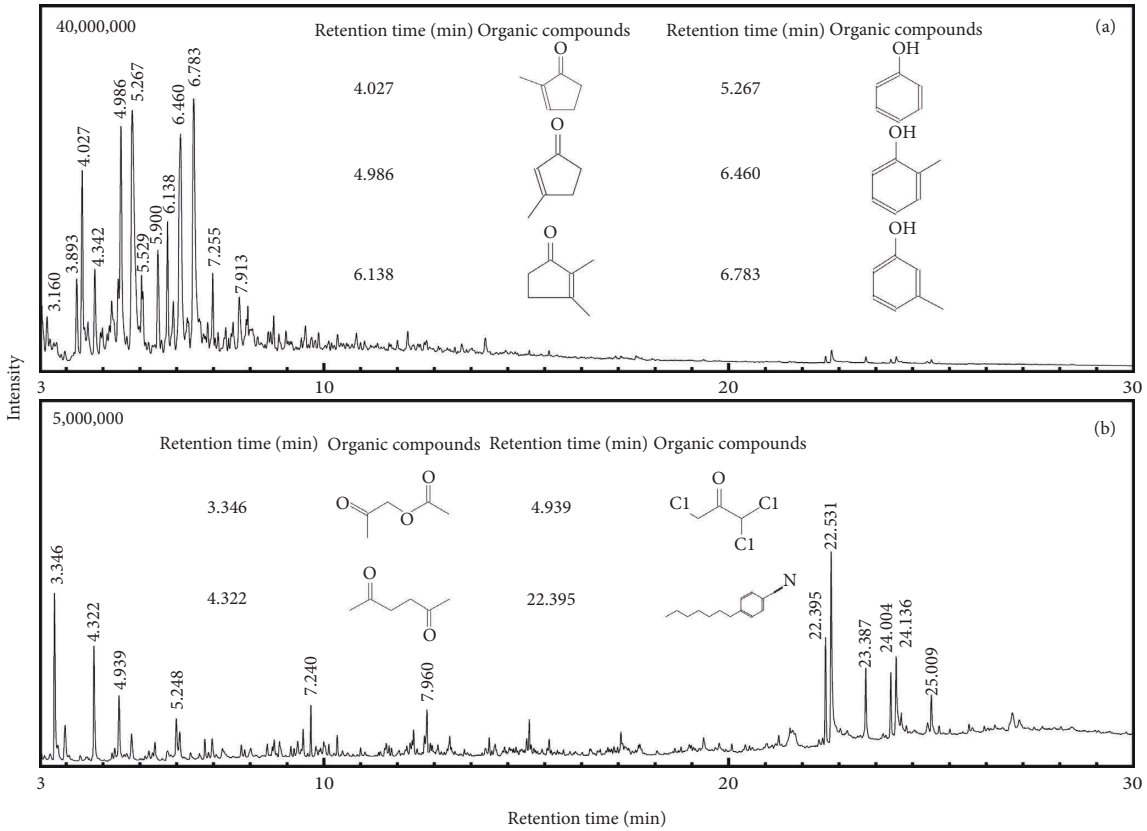

Figure 9: GC-MS total ion chromatogram (TIC) of thermal desorption raw wastewater and Fenton oxidation (FO) effluent.

Table 3: Operating cost statistics.

Unit process	Notes	Operating costs (US$/$m^3$)
DF	Chemical: NaClO, CaCl2, PAC, PAM; lift pump; agitator; sludge pump; reagent delivery pump; mud suction machine	5.55
AS	Chemical: NaOH; agitator; aeration system; air compressor	0.83
FO	Chemical: H2O2, FeSO4•7H2O; agitator; sludge pump; reagent delivery pump; mud suction machine	2.28
RO	Reverse osmosis membrane consumption; reverse osmosis membrane device; drainage pump; reflux pump	0.07
Total expenses	8.73	

and cyclic ketones. Although the organic matter was degraded in the FO stage, the generated organic matter could not be completely mineralized by FO (Figure S5). The remaining organic pollutants present in the raw wastewater and FO effluent are shown in Supplementary Tables S4 and S5, respectively.

3.4. Project Application Evaluation and Benefit Analysis. Based on the data collected in the study and related literature, we compared the cost estimation models of wastewater treatment technology from different authors [51] and found that the cost assessment model of previous studies could not be fully applied to TDW from the actual polluted site of Tahe, Xinjiang, China. For the DF process in this study, the costs mainly include reagents, sludge treatment labor, and maintenance costs, of which the labor cost is estimated to account for about 80%, mainly for sludge treatment [52]. The only disadvantage of the AS process was that it required a large amount of electricity to drive the basic operating equipment, which increase the costs. In the FO process, due to the high COD concentration of wastewater, more hydrogen peroxide in the oxidation stage was consumed, and the cost of chemicals and iron sludge disposal obviously increased. In addition, for the RO membrane process, the costs were mainly composed of four aspects: electricity, chemicals, membrane, and maintenance, of which the electricity costs account for approximately 55% of the total costs, and the maintenance and membrane material costs for 44% [53],

while the labor costs were very low in the membrane treatment [54].

A preliminary estimate of the electricity and chemical costs for each TDW treatment process was made, and the operating costs were listed in Table 3 (see Tables S6-S7 for the main structures and equipment and detailed calculation procedures). Lee et al. [55] in the experiment used the combined process of coagulation-flocculation⟶dissolved air flotation⟶ozonation⟶ultrafiltration⟶reverse osmosis to treat shale-wastewater with a COD of 1250 mg/L up to the standard, and the operation and maintenance costs were 5.91 US$/m^3. Similarly, Xu [56] reported multi effect evaporation⟶microelectrolysis⟶Fenton⟶VTBR-Fenton combined process to treat refractory pesticide wastewater, and the COD of the pesticide wastewater reached up to tens of thousands, and the standard treatment costs were 11.4 US$/m^3. It can thus be seen, the treatment costs for recalcitrant wastewater are generally higher.

4. Conclusions

To solve the potential environmental threat of wastewater from the indirect thermal desorption process, several process schemes were combined. The characteristics and main pollutants of TDW were analyzed, and the removal properties of the unit processes DF, AS, FO, and RO were investigated.

With the DF process, the removal efficiencies of COD, turbidity, and oil content were 15.3%, 97.6%, and 65.3%, respectively. NH_3-N concentration decreased from 204 mg/L to 41 mg/L in the AS process. COD concentration further decreased to 2250 mg/L through the FO process. After RO, COD was less than 150 mg/L. With the combined process, EPH concentration decreased from 818 mg/L to 0.76 mg/L, removal efficiency reached 99.9%. In conclusion, COD and NH_3-N have reached the second-level standard of China's integrated wastewater discharge standard, and petroleum pollutants have reached the first-level standard of China's integrated wastewater discharge standard.

The in-depth analysis of the degradation process of pollutants by UV-vis spectroscopy and EEM fluorescence spectroscopy showed that the FO process effectively removed organic macromolecules, especially aromatic compounds, phenols, and conjugated aldehydes or conjugated ketones. It was further proven by GC-MS that oxidation had an obvious removal effect on phenol and other phenolic compounds and an obvious ring-opening effect on cycloketone and cycloenone.

The engineering applicability and economic analysis of the combined DF⟶AS⟶FO⟶RO process were performed for TDW. The operation and maintenance costs of the combined process were found to be 8.73 US$/m^3, which was higher than the general sewage treatment costs but moderate for recalcitrant wastewater.

Data Availability

The data used to support the findings of this study are included within the supplementary information file(s).

Conflicts of Interest

The authors declare that they have no conflicts of interest.

Acknowledgments

This research was supported by the National Key R&D Program of China (2018YFC1802100).

Supplementary Materials

Figure S1. On-site pictures in Tahe Oilfield, Xinjiang (in order are oil-contaminated soil, soil thermal desorption device, and condensed wastewater). Figure S2. Experimental setup and working schematic diagram for treating TDW. Figure S3. Effect drawing of wastewater treatment in DF process (from left to right, NaClO, CaCl2, PAC, and PAM are added in order). Figure S4. Mass spectra of characteristic pollutants of TDW. Figure S5. Mass spectra of characteristic pollutants of FO effluent. Table.S1. Orthogonal experimental design table for the treatment effect of DF on COD, turbidity, and oil content. Table.S2. Orthogonal experimental design table for the treatment effect of ammonia nitrogen in the AS process. Table.S3. Orthogonal experimental design table for the treatment effect of FO process on COD. Table.S4. Analysis of main organic compounds in TDW. Table.S5. Analysis of main organic compounds in FO effluent. Table.S6. Statistical table of main structures and equipment. Table.S7. Detailed calculation of operating costs. (*Supplementary Materials*)

References

[1] J. W. Liu, K. H. Wei, S. W. Xu et al., "Surfactant-enhanced remediation of oil-contaminated soil and groundwater: a review," *Science of the Total Environment*, vol. 756, 2021.

[2] Mee, "Ministry of ecology and environment of prc) and mls (ministry of land and resources of prc," 2014, https://english.mee.gov.cn/.

[3] C. Zhao, Y. Dong, Y. P. Feng, Y. Z. Li, and Y. Dong, "Thermal desorption for remediation of contaminated soil: a review," *Chemosphere*, vol. 221, pp. 841–855, 2019.

[4] S. Jafarinejad and S. C. Jiang, "Current technologies and future directions for treating petroleum refineries and petrochemical plants (PRPP) wastewaters," *Journal of Environmental Chemical Engineering*, vol. 7, no. 5, 2019.

[5] B. Huang, X. H. Li, W. Zhang, C. Fu, Y. Wang, and S. Fu, "Study on demulsification-flocculation mechanism of oil-water emulsion in produced water from alkali/surfactant/polymer flooding," *Polymers*, vol. 11, no. 3, p. 395, 2019.

[6] S. Verma, B. Prasad, and I. M. Mishra, "Pretreatment of petrochemical wastewater by coagulation and flocculation and the sludge characteristics," *Journal of Hazardous Materials*, vol. 178, no. 1-3, pp. 1055–1064, 2010.

[7] H. Wei, B. Q. Gao, J. Ren, A. M. Li, and H. Yang, "Coagulation/flocculation in dewatering of sludge: a review," *Water Research*, vol. 143, pp. 608–631, 2018.

[8] A. Zangeneh, S. Sabzalipour, A. Takdatsan, R. J. Yengejeh, and M. A. Khafaie, "Ammonia removal form municipal wastewater by air stripping process: an experimental study," *South African Journal of Chemical Engineering*, vol. 36, pp. 134–141, 2021.

[9] C. Cagnetta, B. Saerens, F. A. Meerburg et al., "High-rate activated sludge systems combined with dissolved air flotation enable effective organics removal and recovery," *Bioresource Technology*, vol. 291, 2019.

[10] M. M. Bello, A. A. Abdul Raman, and A. Asghar, "A review on approaches for addressing the limitations of Fenton oxidation for recalcitrant wastewater treatment," *Process Safety and Environmental Protection*, vol. 126, pp. 119–140, 2019.

[11] M. H. Zhang, H. Dong, L. Zhao, D. X. Wang, and D. Meng, "A review on Fenton process for organic wastewater treatment based on optimization perspective," *Science of the Total Environment*, vol. 670, pp. 110–121, 2019.

[12] J. P. Ribeiro and M. I. Nunes, "Recent trends and developments in Fenton processes for industrial wastewater treatment–a critical review," *Environmental Research*, vol. 197, 2021.

[13] S. Ziembowicz and M. Kida, "Limitations and future directions of application of the Fenton-like process in micropollutants degradation in water and wastewater treatment: a critical review," *Chemosphere*, vol. 296, 2022.

[14] D. L. Huang, C. J. Hu, G. M. Zeng et al., "Combination of Fenton processes and biotreatment for wastewater treatment and soil remediation," *Science of the Total Environment*, vol. 574, pp. 1599–1610, 2017.

[15] F. Martínez, R. Molina, I. Rodríguez, M. Pariente, Y. Segura, and J. Melero, "Techno-economical assessment of coupling Fenton/biological processes for the treatment of a pharmaceutical wastewater," *Journal of Environmental Chemical Engineering*, vol. 6, no. 1, pp. 485–494, 2018.

[16] X. Zheng, Z. X. Zhang, D. W. Yu et al., "Overview of membrane technology applications for industrial wastewater treatment in China to increase water supply," *Resources, Conservation and Recycling*, vol. 105, pp. 1–10, 2015.

[17] C. Benito-Alcázar, M. C. Vincent-Vela, J. M. Gozálvez-Zafrilla, and J. Lora-García, "Study of different pretreatments for reverse osmosis reclamation of a petrochemical secondary effluent," *Journal of Hazardous Materials*, vol. 178, no. 1-3, pp. 883–889, 2010.

[18] A. Ullah, H. J. Tanudjaja, M. Ouda, S. W. Hasan, and J. W. Chew, "Membrane fouling mitigation techniques for oily wastewater: a short review," *Journal of Water Process Engineering*, vol. 43, 2021.

[19] M. Tawalbeh, A. Al Mojjly, A. Al-Othman, and N. Hilal, "Membrane separation as a pre-treatment process for oily saline water," *Desalination*, vol. 447, pp. 182–202, 2018.

[20] S. L. Kim, J. Paul Chen, and Y. P. Ting, "Study on feed pretreatment for membrane filtration of secondary effluent," *Separation and Purification Technology*, vol. 29, no. 2, pp. 171–179, 2002.

[21] D. T. Sponza, "Treatment of textile industry wastewater by sequential hybrid processes photo-fenton, ultrafiltration (UF), reverse osmosis (RO) and recovery of some dyes, salt and perfluoroalkyl sulfonate from the retentate," *Journal of Membrane Science and Technology*, vol. 11, no. 2, pp. 1–10, 2020.

[22] https://www.wef.org/resources/publications/books/StandardMethods/.

[23] B. Zhao, L. Y. Ren, Y. B. Du, and J. Wang, "Eco-friendly separation layers based on waste peanut shell for gravity-driven water-in-oil emulsion separation," *Journal of Cleaner Production*, vol. 255, 2020.

[24] M. M. Abdulredha, S. A. Hussain, and L. C. Abdullah, "Optimization of the demulsification of water in oil emulsion via non-ionic surfactant by the response surface methods," *Journal of Petroleum Science and Engineering*, vol. 184, 2020.

[25] R. Yang, H. J. Li, M. Huang, H. Yang, and A. Li, "A review on chitosan-based flocculants and their applications in water treatment," *Water Research*, vol. 95, pp. 59–89, 2016.

[26] R. J. Yao, W. Q. Bian, and T. Dong, "Study on demulsification-Fenton oxidation pretreatment of the mineral oil wastewater," *Coal and Chemical Industry*, vol. 40, pp. 71–75, 2017.

[27] K. K. Das and P. Somasundaran, "Flocculation-dispersion characteristics of alumina using a wide molecular weight range of polyacrylic acids," *Colloids and Surfaces A: Physicochemical and Engineering Aspects*, vol. 223, no. 1-3, pp. 17–25, 2003.

[28] E. J. Kim, H. Kim, and E. Lee, "Influence of ammonia stripping parameters on the efficiency and mass transfer rate of ammonia removal," *Applied Sciences*, vol. 11, no. 1, p. 441, 2021.

[29] K. Emerson, R. C. Russo, R. E. Lund, and R. V. Thurston, "Aqueous ammonia equilibrium calculations: effect of pH and temperature," *Journal of the Fisheries Research Board of Canada*, vol. 32, no. 12, pp. 2379–2383, 1975.

[30] J. J. Pignatello, E. Oliveros, and A. MacKay, "Advanced oxidation processes for organic contaminant destruction based on the Fenton reaction and related chemistry," *Critical Reviews in Environmental Science and Technology*, vol. 36, no. 1, pp. 1–84, 2006.

[31] J. L. Wang and J. T. Tang, "Fe-based Fenton-like catalysts for water treatment: catalytic mechanisms and applications," *Journal of Molecular Liquids*, vol. 332, 2021.

[32] B. Jain, A. K. Singh, H. Kim, E. Lichtfouse, and V. K. Sharma, "Treatment of organic pollutants by homogeneous and heterogeneous Fenton reaction processes," *Environmental Chemistry Letters*, vol. 16, no. 3, pp. 947–967, 2018.

[33] T. V. Huu, H. N. Lan, and K. H. Trung, "Heterogeneous Fenton oxidation of paracetamol in aqueous solution using iron slag as a catalyst: Degradation mechanisms and kinetics," 2020, https://www.sciencedirect.com/science/article/pii/S2352186419308983.

[34] A. K. Hassan, M. M. Abdul Hassan, A. F. Hasan, and A. F. Hasan, "Treatment of Iraqi petroleum Refinery wastewater by advanced oxidation processes," *Journal of Physics: Conference Series*, vol. 1660, no. 1, 2020.

[35] C. J. Liu, G. Y. Dong, T. Tsuru, and H. Matsuyama, "Organic solvent reverse osmosis membranes for organic liquid mixture separation: a review," *Journal of Membrane Science*, vol. 620, 2021.

[36] J. S. Huwaidi, M. A. Obaidi, and A. T. Jarullah, "Modelling and simulation of a hybrid system of trickle bed reactor and multistage reverse osmosis process for the removal of phenol from wastewater," 2021, https://www.sciencedirect.com/science/article/abs/pii/S0098135421002301.

[37] A. Pozderović, T. Moslavac, and A. Pichler, "Influence of processing parameters and membrane type on permeate flux during solution concentration of different alcohols, esters, and aldehydes by reverse osmosis," *Journal of Food Engineering*, vol. 78, no. 3, pp. 1092–1102, 2007.

[38] L. O. Guzmán, D. M. C. Cuevas, and T. A. Martínez, "Fenton-biostimulation sequential treatment of a petroleum-contaminated soil amended with oil palm bagasse," *Chemistry and Ecology*, vol. 37, no. 6, pp. 573–588, 2021.

[39] Y. Ma, H. Z. Zhao, and M. D. Yu, "Spectral parameter method for rapid identification of water characteristics of petroleum hydrocarbon contaminated sites," *Spectroscopy and Spectral Analysis*, vol. 41, pp. 822–827, 2021.

[40] J. L. Weishaar, G. R. Aiken, B. A. Bergamaschi, M. S. Fram, R. Fujii, and K. Mopper, "Evaluation of specific ultraviolet absorbance as an indicator of the chemical composition and reactivity of dissolved organic carbon," *Environmental Science and Technology*, vol. 37, no. 20, pp. 4702–4708, 2003.

[41] Y. P. Lee, M. Fujii, K. Terao, T. Kikuchi, and C. Yoshimura, "Effect of dissolved organic matter on Fe(II) oxidation in natural and engineered waters," *Water Research*, vol. 103, pp. 160–169, 2016.

[42] L. Zhang, K. C. Xu, S. R. Wang et al., "Characteristics of dissolved organic nitrogen in overlying water of typical lakes of Yunnan Plateau, China," *Ecological Indicators*, vol. 84, pp. 727–737, 2018.

[43] F. Shi, T. T. Mao, Y. T. Cao et al., "Morphological grayscale reconstruction and ATLD for recognition of organic pollutants in drinking water based on fluorescence spectroscopy," *Water*, vol. 11, no. 9, p. 1859, 2019.

[44] Y. Z. Lu, N. Li, Z. W. Ding et al., "Tracking the activity of the Anammox-DAMO process using excitation–emission matrix (EEM) fluorescence spectroscopy," *Water Research*, vol. 122, pp. 624–632, 2017.

[45] E. I. Karavanova, A. G. Konovalov, and E. V. Terskaya, "Applying the method of fluorescence spectroscopy to study dissolved organic matter in waters of the moskva river," *Moscow University Soil Science Bulletin*, vol. 74, no. 5, pp. 199–207, 2019.

[46] B. Lai, Y. X. Zhou, J. L. Wang, Z. Yang, and Z. Chen, "Application of excitation and emission matrix fluorescence (EEM) and UV–vis absorption to monitor the characteristics of Alizarin Red S (ARS) during electro-Fenton degradation process," *Chemosphere*, vol. 93, 2013.

[47] I. Sciscenko, A. Arques, P. Micó, M. Mora, and S. Garcia-Ballesteros, "Emerging applications of EEM-PARAFAC for water treatment: a concise review," *Chemical Engineering Journal Advances*, vol. 10, 2022.

[48] 肖. Xiao Chang-jiang and 张. Zhang Jing-chao, "Multiple peak calibration of gasoline-in-water concentration measurement using three-dimensional fluorescence spectra," *Chinese Journal of Luminescence*, vol. 38, no. 10, pp. 1391–1402, 2017.

[49] M. V. Bosco and M. S. Larrechi, "PARAFAC and MCR-ALS applied to the quantitative monitoring of the photodegradation process of polycyclic aromatic hydrocarbons using three-dimensional excitation emission fluorescent spectraComparative results with HPLC," *Talanta*, vol. 71, no. 4, pp. 1703–1709, 2007.

[50] R. Z. Xu, J. S. Cao, and G. Y. Feng, "Fast identification of fluorescent components in three-dimensional excitation-emission matrix fluorescence spectra via deep learning," *Chemical Engineering Journal*, vol. 430, 2022.

[51] P. L. Gurian, M. J. Small, J. R. Lockwood, and M. J. Schervish, "Benefit-cost estimation for alternative drinking water maximum contaminant levels," *Water Resources Research*, vol. 37, no. 8, pp. 2213–2226, 2001.

[52] F. El-Gohary, A. Tawfik, and U. Mahmoud, "Comparative study between chemical coagulation/precipitation (C/P) versus coagulation/dissolved air flotation (C/DAF) for pretreatment of personal care products (PCPs) wastewater," *Desalination*, vol. 252, no. 1-3, pp. 106–112, 2010.

[53] J. R. Sharma, M. Najafi, and S. R. Qasim, "Preliminary cost estimation models for construction, operation, and maintenance of water treatment plants," *Journal of Infrastructure Systems*, vol. 19, no. 4, pp. 451–464, 2013.

[54] B. Valizadeh, F. Zokaee Ashtiani, A. Fouladitajar et al., "Scale-up economic assessment and experimental analysis of MF–RO integrated membrane systems in oily wastewater treatment plants for reuse application," *Desalination*, vol. 374, pp. 31–37, 2015.

[55] Y. Lee, M. C. Cui, J. Choi, Y. Jeong, and J. Khim, "Demonstration and evaluation of potential configuration options for shale-wastewater treatment plant by combining several unit processes," *Journal of Cleaner Production*, vol. 232, pp. 867–876, 2019.

[56] C. K. Xu, *Study and Application on Treatment of Pesticide Wastewater by Combined Process of Multi Effect Evaporation—Mrico-Electrolysis—Fenton—VTBR-Fenton Technology*, Dalian university of Technology, Dalian, China, 2017.